

Lab on a Chip

Accepted Manuscript



This is an *Accepted Manuscript*, which has been through the Royal Society of Chemistry peer review process and has been accepted for publication.

Accepted Manuscripts are published online shortly after acceptance, before technical editing, formatting and proof reading. Using this free service, authors can make their results available to the community, in citable form, before we publish the edited article. We will replace this *Accepted Manuscript* with the edited and formatted *Advance Article* as soon as it is available.

You can find more information about *Accepted Manuscripts* in the [Information for Authors](#).

Please note that technical editing may introduce minor changes to the text and/or graphics, which may alter content. The journal's standard [Terms & Conditions](#) and the [Ethical guidelines](#) still apply. In no event shall the Royal Society of Chemistry be held responsible for any errors or omissions in this *Accepted Manuscript* or any consequences arising from the use of any information it contains.



Journal Name

ARTICLE

Cell-sized condensed collagen microparticles for preparing microengineered composite spheroids of primary hepatocytes

Masumi Yamada,^{a,*} Ayaka Hori,^a Sari Sugaya,^a Yuya Yajima,^a Rie Utoh,^b Masayuki Yamato,^b and Minoru Seki^a

Received 00th January 20xx,
Accepted 00th January 20xx

DOI: 10.1039/x0xx00000x

www.rsc.org/

The reconstitution of extracellular matrix (ECM) components in three-dimensional (3D) cell culture environments with microscale precision is a challenging issue. ECM microparticles would potentially be useful as solid particulate scaffolds that can be incorporated into 3D cellular constructs, but technologies for transforming ECM proteins into cell-sized stable particles are currently lacking. Here, we describe new processes to produce highly condensed collagen microparticles by means of droplet microfluidics or membrane emulsification. Droplets of an aqueous solution of type I collagen were formed in a continuous phase of polar organic solvent, followed by rapid dissolution of water molecules into the continuous phase because the droplets were in a non-equilibrium state. We obtained highly unique, disc-shaped condensed collagen microparticles with a final collagen concentration above 10%, and examined factors affecting particle size and morphology. After testing the cell-adhesion properties on the collagen microparticles, composite multicellular spheroids comprising the particles and primary rat hepatocytes were formed using microfabricated hydrogel chambers. We found that the ratio of the cells and particles is critical in terms of improvement of hepatic functions in the composite spheroids. The presented methodology for incorporating particulate-form ECM components in multicellular spheroids would be advantageous because of the biochemical similarity with the microenvironments in vivo.

Introduction

The construction of 3D cellular environments mimicking in vivo tissues is thought to be beneficial in preserving/regulating cellular functions and differentiation, analyzing cellular responses to drugs and toxins, and preparing artificial tissues for transplantation therapy. Among the various technologies used to realize cell culture in 3D, the formation of a multicellular spheroid is a highly effective, simple, and easy-to-perform strategy to assemble cells into a compact and closely packed configuration, taking advantage of the inherent tendency of cells to aggregate¹. Various techniques have been developed to form multicellular spheroids, for example, using round-bottom microwells², hanging drop plates³, microfabricated chambers^{4,5}, microfluidic devices⁶⁻⁸, and patterned cell adhesive/non-adhesive surfaces^{9,10}. Non-cell-adhesive surfaces have been employed for most of these substrates; in such a cell culture environment where cell-to-surface contacts are limited, cells are forced to adhere with other surrounding cells, forming cell-cell connections in a 3D format. Spheroid-based cultivation, for example, is frequently utilized for preparing embryoid bodies of ES cells, where

efficient control of cell differentiation is achieved¹¹⁻¹³. Hepatocellular spheroids are expected to be useful tools for evaluating drug metabolism at the initial stage of drug screening, because hepatic functions are maintained for a relatively long time period owing to the in vivo tissue-like configuration^{2,4,14}. Various forms of multicellular spheroids have been prepared, including neurospheres¹⁵, pancreatic islet-like tissues^{16,17}, and 3D tumor models¹⁸⁻²². In addition, the preparation of heterotypic spheroids/aggregates, which potentially reproduce the considerable cellular heterogeneity of in vivo tissues and organs, has drawn great attention^{2,14,23-25}. Furthermore, multicellular spheroids have been utilized not only for reproducing in vivo cellular environments but also for constructing large tissue models through assembly of spheroids as unit structures^{26,27}.

Despite the high utility and versatility of multicellular spheroids, a methodology for reconstituting extracellular matrix (ECM) components with micrometer-scale precision in such closely packed constructs is currently lacking. For example, in epithelial tissues, cells contact ECM components in the basal membrane, and the cell-cell and cell-ECM interactions harmonize with each other to support cell survival, proliferation, differentiation, and polarity. In a typical spheroid culture, cell-ECM interactions are not properly formed until secreted ECM components from spheroid-composing cells accumulate; the absence of ECM components would be problematic, especially for epithelial cells that do not sufficiently produce ECM components, including

^a Department of Applied Chemistry and Biotechnology, Graduate School of Engineering, Chiba University, 1-33 Yayoi-cho, Inage-ku, Chiba 263-8522, Japan.
*m-yamada@faculty.chiba-u.jp

^b Institute of Advanced Biomedical Engineering and Science, Tokyo Women's Medical University, 8-1 Kawada-cho, Shinjuku-ku, Tokyo 162-8666, Japan.

hepatocytes²⁸. We hypothesized that if ECM molecules were transformed into cell-sized solid microparticles, they would be useful as particulate scaffolds that could be stably incorporated into multicellular spheroids. Such spheroids would not only be able to realize the cell-cell interactions but also enhance the cell-matrix interactions with microscale uniformity, and would be advantageous in maintaining/regulating cellular functions, such as differentiation, network formation, and migration.

Several attempts have been made to produce microparticles made of collagen²⁹⁻³². Most previous methods employed bulk-scale emulsification techniques for producing collagen particles from a diluted collagen solution (initial concentration typically lower than 1%). The particles obtained were used as, for example, growth-factor-loading biocompatible carriers for controlled delivery^{29,30}. In addition, microfluidic devices have been used to produce collagen hydrogel microbeads with an average size greater than ~ 100 μm , large enough to encapsulate living cells^{27,33}. Nevertheless, to our knowledge, the formation of multicellular spheroids incorporating particles made of ECM proteins, including collagen, has not been reported, and the application of collagen particles is limited. This is likely due to a combination of factors, including the relatively poor physical stability of the particles, the possible denaturation of collagen molecules, and the unsuitable processing conditions for collagen microparticles³⁴.

We recently developed a process to produce monodisperse, single micrometer-sized particles made of natural/synthetic polymers by using droplets in a non-equilibrium state formed in microfluidic devices^{35,36}. This process begins by forming droplets of an aqueous solution of precursor molecules in a continuous phase of water-soluble polar organic solvent, such as methyl acetate. Because of the dissolution of the water molecules from the droplets, the precursor molecules are greatly condensed within the droplet, forming solid particles with a final size significantly smaller than that of the droplets at the time of formation. In the present study, we applied this process to the production of type I collagen microparticles. In addition to the microfluidic technology, a membrane-emulsification process was adopted for the mass production of collagen particles. We examined several factors affecting the size and shape of the collagen particles. As an application of the particles, we have demonstrated the formation of collagen particles incorporating composite spheroids using primary rat hepatocytes, in an attempt to evaluate the effectiveness of the ECM components transformed into particulate formats for improving hepatocellular functions.

Experimental

Fabrication of microfluidic devices

Microfluidic devices made of polydimethylsiloxane (PDMS) were fabricated using soft lithography and replica molding processes, as described previously³⁷. In brief, microstructures

of a negative photoresist (SU-8 3050, Nippon Kayaku, Tokyo, Japan) were patterned on a silicon wafer through photolithography, after which PDMS prepolymer (Silpot 184, Dow Corning Toray, Tokyo, Japan) was poured onto this master mold and cured at 85°C for 30 min. After completing the crosslinking reaction, the PDMS replica was peeled off from the mold and through-holes for inlets/outlets were made by punching. This PDMS plate with the channel structure and a flat PDMS plate were bonded via O₂ plasma treatment using a plasma reactor (PR500, Yamato Scientific, Tokyo, Japan). Silicone tubes with inner/outer diameters of 1/2 mm, respectively, were attached to the inlet/outlet holes, and glued. To ensure that the microchannel surface was completely hydrophobic, the microfluidic device was heated at 150°C in a convection oven for at least 3 h before use.

The microchannel design used to produce collagen microparticles is shown in Fig. 1 (A, B). There are four inlets: Inlet 1 was used for introducing the polar organic solvent; Inlet 2 for the aqueous solution of collagen; and Inlets 3 and 3' for the aqueous solution of crosslinking reagent. The width of the microchannel was 200 μm throughout, excluding the orifice for droplet generation (50 μm). The depth of the entire microchannel was uniform at ~ 55 μm . The length of the droplet dissolution channel was 70 mm, and that of the crosslinking channel was 75 mm.

Production of collagen microparticles using microfluidic devices

An aqueous solution of collagen was prepared by diluting type I collagen solution (from the rat tail tendon, concentration of 9–12 mg/mL, BD Biosciences, CA, USA) with an aqueous solution of 0.02 M acetic acid. The final collagen concentration was changed from 0.01% (0.1 mg/mL) to 0.2% (2 mg/mL). The crosslinking reagent was prepared by diluting a glutaraldehyde solution (25%, Wako Pure Chemical, Osaka, Japan) with Dulbecco's phosphate-buffered saline (PBS, Takara Bio, Shiga, Japan); the final glutaraldehyde concentration was 2.5%. Methyl acetate (purity > 98%, Wako), the collagen solution, and the crosslinking reagent were continuously introduced into the microchannel using syringe pumps (KDS200, KD Scientific, MA, USA) from Inlets 1, 2, and 3 and 3', respectively, with flow rates of Q_1 , Q_2 , and Q_3 ($=Q_{3'}$), respectively. The generation behaviors of droplets/particles were observed using an inverted optical microscope (IX71, Olympus, Tokyo, Japan) and a CCD camera (DP72, Olympus). The collagen particles prepared were collected in a glass vial containing PBS with 2.5% glutaraldehyde. The particles were then washed thrice with Dulbecco's modified Eagle medium (DMEM, Sigma-Aldrich, MO, USA) supplemented with 10% fetal bovine serum (FBS, Life Technologies, CA, USA) via centrifugation to completely remove the remaining glutaraldehyde. The size of the droplets/particles was measured by analyzing 100~200 droplets/particles via image processing for each condition; the shortest and longest axes were averaged for incompletely spherical particles.

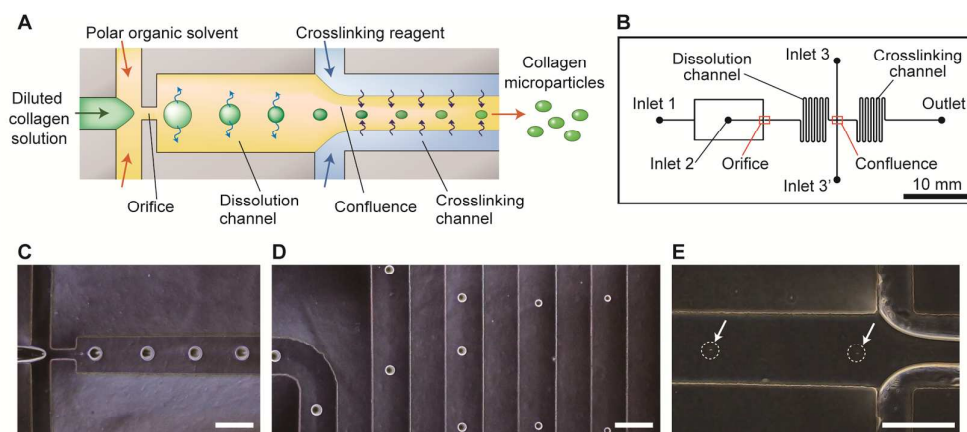


Figure 1. (A) Schematic illustration showing the microfluidic process for producing collagen microparticles. (B) Microchannel design used to produce collagen microparticles. (C–E) Collagen droplets in a non-equilibrium state formed at the orifice and shrinking in the microchannel. (C) Droplets near the orifice. (D) Droplet flowing through the dissolution channel. (E) Completely shrunk and condensed collagen particles entering the confluence point. Scale bar, 200 μm .

Production of collagen microparticles using membrane emulsification

Porous membranes made of Shirasu porous glass with hydrophobic surface properties and with different pore sizes (pore sizes of 5 μm , 10 μm , and 20 μm ; SPG direct connector, SPG Technology, Miyazaki, Japan) were employed. As a continuous phase, 75 mL of methyl acetate was poured into a 200 mL beaker and was vigorously stirred using a magnetic stirrer. A 0.1% type I collagen solution in 0.02 M acetic acid was continuously pumped into the continuous phase of methyl acetate through the porous membrane, which was dipped in the continuous phase, at a feeding speed of 0.1 mL/min using the syringe pump. After introducing ~ 5 mL of the collagen solution, 5 mL of 2.5% glutaraldehyde solution was added to the beaker and gently stirred for 15 min. The prepared collagen particles partitioned in the aqueous phase were collected in a plastic tube and then washed thrice with DMEM with FBS via centrifugation.

Characterization of collagen particles

First, the particle morphologies were observed by scanning electron microscopy (SEM). The particles obtained using microfluidic devices were washed with distilled water, and then a small aliquot of the particle suspension was dropped onto a conductive carbon tape and dried. After sputtering a thin Au layer using a sputtering device (MSP-1S, Shinku Device, Ibaraki, Japan), the surface morphology of the particles was observed by scanning electron microscopy (SEM; VE-8800, Keyence, Tokyo, Japan). Next, the inner microstructures of the particles were observed by freeze fracture transmission electron microscopy (FF-TEM). Briefly, the particles prepared by the membrane emulsification were concentrated in 50% (v/v) ethanol in water, and frozen using slush nitrogen. A flat section was prepared and then water and ethanol were sublimed under vacuum at -90°C using a freeze fracture system (JFD-V, JEOL, Tokyo, Japan). Thin Pt and carbon layers were deposited stepwise on the section, and the surface

micropatterns were transferred to the thin Pt/carbon film. This replica was moved to a TEM grid, and examined for the TEM analysis (JEM-1010, JEOL). The black/white patterns of the captured images were digitally reversed. In addition to the SEM/TEM observations, the particles were dipped in DMEM containing ~ 700 U/mL collagenase L (from *Streptomyces parvulus*, Wako), to examine their enzymatic degradability. The morphology of the microparticles was observed using inverted microscopy.

Cell adhesion test

NIH-3T3 cells and HepG2 cells (both supplied from Riken BioResource Center, Ibaraki, Japan) were maintained in DMEM supplemented with 10% FBS, 0.1 mg/mL streptomycin, and 100 U/mL penicillin (Sigma) under 20% O_2 and 5% CO_2 at 37°C in a CO_2 incubator. Cells were harvested from dishes via trypsin-EDTA (Sigma) treatment and washed with the cell culture medium. Fluorescent collagen particles were produced using microfluidic devices; FITC-labeled type I collagen (Collagen Research Center, Tokyo, Japan) was added to non-labeled collagen at a ratio of 1:10. The collagen particles obtained and cells were suspended in the cell culture medium at concentrations of 6×10^4 particles/mL and 2×10^5 cells/mL, respectively, and then 2.5 mL of the cell/particle suspension was introduced into a 35-mm non-cell-adhesive culture dish (Hydrocell, Cell Seed, Tokyo, Japan). The dish was gently shaken with a rotating shaker in a CO_2 incubator. Cell nuclei were stained with Hoechst 33342 dye (Life Technologies), and the morphology of the cell/particle complex was observed using fluorescence microscopy.

Formation of composite spheroids of primary rat hepatocytes

Non-cell-adhesive microchambers made of agarose hydrogel were employed for preparing heterogeneous spheroids composed of cells and collagen particles. First, circular posts made of SU-8 3050 were patterned on silicon wafers using photolithography; a silicon mold (20 \times 20 mm) was prepared

with 32×32 (1,024 arrays) of 200- μm circular posts with a height of $\sim 300 \mu\text{m}$ and a distance between each post of 300 μm . After placing the silicon mold in a 60-mm dish, $\sim 2 \text{ mL}$ of an aqueous solution of 3% agarose I (Dojindo Corp., Kumamoto, Japan) and 0.9% NaCl was poured onto the mold. Subsequently, it was gelled by incubating at 4°C for 30 min. The gelled agarose plate with microchamber structures was peeled off from the mold and dipped in a serum-free medium for hepatocyte culture (Williams' Medium E, Life Technologies, with supplements²⁴) for at least 1 day before being used for experiments.

All animal experiments were performed with the approval of the Institutional Animal Care and Use Committee of Tokyo Women's Medical University. Hepatocytes were isolated from 8- to 10-week-old male F344/NSlc rats (Japan SLC, Shizuoka, Japan), using the collagenase perfusion procedure as described previously³⁸. The hepatocytes obtained were purified by density centrifugation using Percoll. Cells with an initial viability greater than $\sim 85\%$ were used. Collagen particles, prepared using membrane emulsification with addition of 0.01% FITC-labeled collagen, and hepatocytes were mixed at different ratios (particles:cells = 1:1 and 4:1) and were seeded into the hydrogel microchambers. Cells were cultured in the serum-free culture medium under a high O_2 tension condition (90%) for the first 24 h of cultivation and then under a standard O_2 condition (20%) for up to 14 days. As negative controls, hepatocytes were cultured at a density of 7×10^4 cells/ cm^2 on type I collagen-coated 60-mm dishes (Asahi Techno Glass, Tokyo, Japan) and spheroids were formed without incorporating collagen particles. The spheroids obtained were observed using an inverted optical/fluorescence microscope.

Immunofluorescence staining

Formed spheroids were retrieved from the microchambers via gentle centrifugation. Recovered spheroids were embedded in OCT compound (Sakura Finetek, Tokyo, Japan) and frozen at -80°C . Frozen 8- μm -thick sections were prepared using a cryostat (LEICA CM1510S, Leica Biosystems, Wetzlar, Germany), which were then fixed on glass slides (S9441, MAS coat, Matsunami Glass, Osaka, Japan) with 4% paraformaldehyde (Wako) for 5–10 min and incubated in PBS for 5–10 min at room temperature. After rinsing with PBS containing 10% donkey serum (Life Technologies), the sections were incubated with sheep polyclonal antibodies against rat albumin (anti albumin; Bethyl Laboratories, Montgomery, TX, USA) to stain hepatocytes. The sections were rinsed with PBS and incubated for 30 min with Alexa Fluor 594-conjugated anti-sheep IgG secondary antibodies (Life Technologies). The nuclei of hepatocytes were stained with 4, 6-diamidino-2-phenylindole (DAPI, Life Technologies).

Gene expression analysis by real-time RT-PCR

TRIzol Reagent (Life Technologies) and a PureLink RNA Mini Kit (Life Technologies) were used to isolate total RNA by columnar centrifugation. DNase I (Life Technologies) was used to

completely eliminate genomic DNA. Complementary DNA was synthesized from 100 ng of total RNA using SuperScript III reverse transcriptase (Life Technologies). Quantitative real-time reverse transcription polymerase chain reaction (qPCR) was performed with Taqman expression assays (Life Technologies) according to the manufacturer's instructions using the StepOne Plus Real-time PCR System (Life Technologies) for the following genes: ATP synthase subunit b, mitochondrial (*ATP5F1*), albumin (*ALB*), ornithine transcarbamylase (*OTC*), and cytochrome P450, family 3, subfamily a, polypeptide 23/polypeptide 1 (*CYP3A1*). Relative gene expression was quantified with the comparative C_T method, using *ATP5F1* as the internal control. Results are shown as the mean \pm SD from six individual samples. Results were analyzed by one-way analysis of variance (ANOVA) with Tukey's honest significance difference test (HSD) or the Bonferroni post hoc test using IBM SPSS Statistics 22 software (IBM Japan, Tokyo, Japan). A value of P less than 0.05 was considered statistically significant.

Results

Production of collagen microparticles using microfluidic devices

We previously produced micrometer-sized hydrogel beads by the dissolution of droplets in a non-equilibrium state and subsequent concentration and precipitation of polymer molecules³⁵. In this study, we applied this approach to the production of cell-sized concentrated collagen particles. We first observed the formation and dissolution behaviors of droplets of a collagen solution in a microfluidic device. Figure 1 (C–E) shows the droplets in the microchannel, when the inlet flow rates Q_1 , Q_2 , Q_3 were 30, 0.9, 15, and 15 $\mu\text{L}/\text{min}$, respectively, and the initial collagen concentration was 0.1%. Highly monodisperse droplets with diameters of $72.4 \mu\text{m} \pm 2.5 \mu\text{m}$ (average \pm SD; CV of 3.5%) were generated at the orifice, with a corresponding droplet volume of $\sim 200 \text{ pL}$. The production rate of droplets was ~ 150 droplets/s. While flowing through the droplet dissolution channel, water molecules in the droplet dissolved into the continuous phase of methyl acetate and collagen molecules were concentrated. At the confluence point, where the retention time was $\sim 1.5 \text{ s}$, the droplet shrinkage was completed and the final droplet diameter was $\sim 10 \mu\text{m}$ (Fig. 1 (E)). The concentrated droplets then entered the crosslinking channel, where the collagen molecules became chemically crosslinked. The crosslinking solution and the continuous phase of methyl acetate formed a parallel laminar flow. The collagen molecules were crosslinked and formed stable particles, possibly because of the diffusion-based supply of glutaraldehyde to the concentrated droplets. It should be noted that particle aggregates were formed not when crosslinking solution was introduced into the microchannel, but when it was added into the outer glass vial.

The collagen particles obtained when the initial collagen concentration was changed from 0.01% to 0.2% are shown in Figure 2. Under these conditions, the particles exhibited unique erythrocyte-like morphologies. The particle size

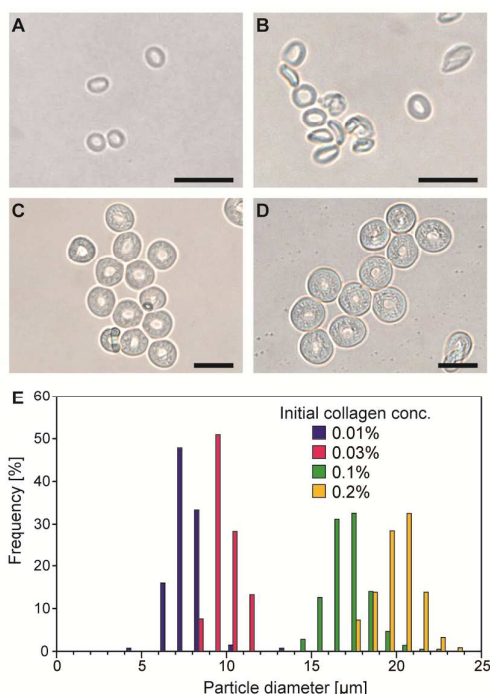


Figure 2. (A–D) Collagen microparticles prepared using microfluidic devices. The initial collagen solutions were (A) 0.01%, (B) 0.03%, (C) 0.1%, and (D) 0.2%, respectively. (E) Size distributions of collagen particles. Scale bar, 20 μm .

increased with the increase of the initial collagen concentration, while the particle morphology did not change significantly. The distributions of the particle diameter are shown in Fig. 2 (E). When the initial collagen concentration was 0.1%, the average diameter \pm SD of the disc-like particles was $17.0 \mu\text{m} \pm 1.2 \mu\text{m}$ (with a CV value of 7.3%), whereas the thickness was $8.0 \mu\text{m} \pm 1.2 \mu\text{m}$, indicating that the shape and the size of the particles were uniform. This unique morphology was likely the result of the formation and subsequent deformation of a shell structure during the droplet dissolution process. Because collagen molecules are not soluble in the continuous phase, they are concentrated on the droplet surface, forming a relatively solid shell structure. This shell structure is then deformed by further droplet shrinkage, resulting in the formation of disc-like particles. Assuming that the particle is composed of a toroidal rim and a planar central column, particle volume was estimated to be $\sim 1.5 \text{ pL}$ for the particles prepared using 0.1% collagen solution. Based on this estimate, we theorized that the collagen molecules were greatly concentrated, with a final concentration in the particle of $\sim 14\%$. Similar values were obtained for particles prepared under different collagen concentration conditions. It is notable that treatment with glutaraldehyde did not affect the particle size.

Next, we investigated the effect of the production condition on particle morphology. The total flow rate of the solutions introduced was changed from ~ 30 to $\sim 120 \mu\text{L}/\text{min}$, whereas the ratio of the flow rates was kept constant ($Q_1:Q_2:Q_3=1:0.03:0.5:0.5$). As shown in Fig. 3 (A), relatively thick, disc-shaped particles were generated when the flow rate

was low (Q_1 of $15 \mu\text{L}/\text{min}$). By contrast, thinner particles were formed under a higher flow rate condition (Q_1 of $60 \mu\text{L}/\text{min}$). This may be attributed to the difference in the thickness of the collagen film formed on the droplet surface under different flow rates. We estimated the dissolution speed of droplets under different flow rate conditions by measuring droplet volumes at different points in the microchannel, as shown in Fig. 3 (C). Although the initial droplet sizes were almost unchanged, the time points at which the droplet volumes became 10% of the initial value differed (~ 660 , ~ 580 , and ~ 470 ms for Q_1 of 15, 30, and $60 \mu\text{L}/\text{min}$, respectively, as estimated from the fitting curves based on exponential decay drawn by the least squares method). This result indicates that higher flow rates resulted in the faster dissolution of droplets, which may have caused the formation and subsequent deformation of a relatively thin but solid surface film and the formation of thinner disc-shaped particles.

Production of collagen microparticles using membrane emulsification

Microfluidic technology can be used to produce highly monodisperse, cell-sized collagen microparticles. However, the production speed is only $\sim 6 \times 10^5$ particles/h, which is sometimes insufficient when they are used as scaffolds for cell cultivation. Hence, we employed another technique, membrane emulsification, to improve the production throughput (Fig. 4 A). To produce water-in-oil (w/o) droplets, porous glass membranes with a hydrophobic surface and with different pore sizes (5, 10, and $20 \mu\text{m}$) were used. Figure 4 (B–D) shows the particles obtained. The average diameters \pm SD were 5.5 ± 1.7 , 9.5 ± 2.8 , and $16.5 \pm 5.4 \mu\text{m}$, respectively, when membranes with pore sizes of 5, 10, and $20 \mu\text{m}$ were used. On

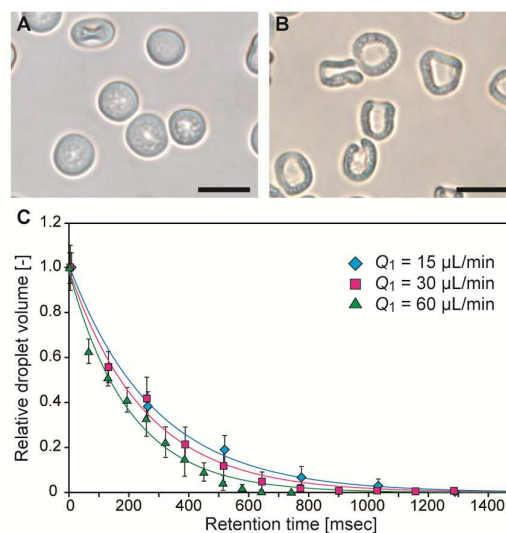


Figure 3. Control of collagen particle morphology by changing the total flow rate while keeping the flow rate ratio constant. The total flow rates of the continuous phase of methyl acetate were (A) $15 \mu\text{L}/\text{min}$ and (B) $60 \mu\text{L}/\text{min}$, respectively. Scale bar, $20 \mu\text{m}$. (C) Time course change in the droplet volume when the total flow rate was changed.

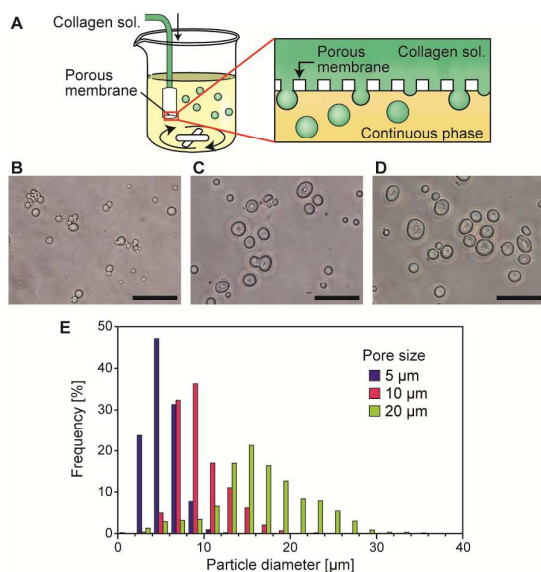


Figure 4. (A) Schematic showing the collagen particle production using membrane emulsification. (B–D) Collagen microparticles obtained by using porous membranes with different pore sizes: (B) 5 μm, (C) 10 μm, and (D) 20 μm. Scale bar, 50 μm. (E) Size distributions of the collagen particles.

comparison with the droplet/particle-size relationship in the microfluidic experiments, it was deduced that droplets with initial sizes ~ 4 times larger than the pore size were produced, which then shrunk to form particles. This estimation is consistent with the literature that generally droplets with sizes 3–5 times larger than the pore sizes are formed with conventional membrane emulsification techniques³⁹. The particles formed showed similar disc-like morphology as in the case of the microfluidic process, but there were some particle aggregates, which were possibly formed by coalescence of multiple droplets during the dissolution and/or crosslinking process. The size distributions of the particles are shown in Fig. 4 (E). Although the size distribution was relatively large (CV of $\sim 30\%$) as compared to that of the particles produced by the microfluidic process, the production speed of the particles dramatically increased (e.g., $\sim 3.5 \times 10^7$ particles/h for the 10-μm membranes), showing the superiority of the process in terms of large-scale production.

Characterization of collagen microparticles

The surface morphology of the particles obtained was examined by SEM. Figure 5 (A, B) shows SEM images of the dried collagen particles on a conductive carbon tape. The particle surface was rough, likely due to the accumulation of fibrous collagen. The cross sectional images of the particle observed by FF-TEM are shown in Figure 5 (C, D). It was revealed that the internal structure was consisted of randomly orientated collagen fibers with diameters of 10–20 nm, and the particles were uniformly packed with condensed collagen fibers. Additionally, we tested the enzymatic degradability of the particles by treating them with collagenase. The collagen

particles were digested and dissolved in the aqueous solution of collagenase after 8 h of incubation at 25°C (Fig. 5 E, F).

Cell cultivation on collagen particles

To examine the cell adhesion capabilities of the collagen particles obtained, two types of cells were cultured with the particles using suspension cultivation. Figure 6 shows NIH-3T3 cells and HepG2 cells on a non-cell-adhesive dish cultured with the fluorescent collagen microparticles prepared using microfluidic devices. Both types of cells adhered on the surface of the collagen particles within several hours of cultivation. Cell-particle aggregates were formed, especially by the highly adhesive NIH-3T3 cells, as these cells acted as a binder between particles. In addition, cells tended to adhere on both sides of the particles due to the disc-like morphology of the particles. These results clearly show the applicability of collagen particles as particulate scaffolds for cell culture purposes.

Formation of composite spheroids of primary hepatocytes

Next, we prepared composite spheroids of primary rat hepatocytes incorporating collagen particles, as shown in Fig. 7. Particles were prepared from 0.1% collagen solution with 0.01% FITC collagen using membrane emulsification with a 10 μm-pore membrane. The average particle size was ~ 10 μm, which was smaller than primary hepatocytes (20–30 μm in size). The ratio of cells to particles was changed between 1:1 and 1:4 in order to examine the effects of the cell-matrix and

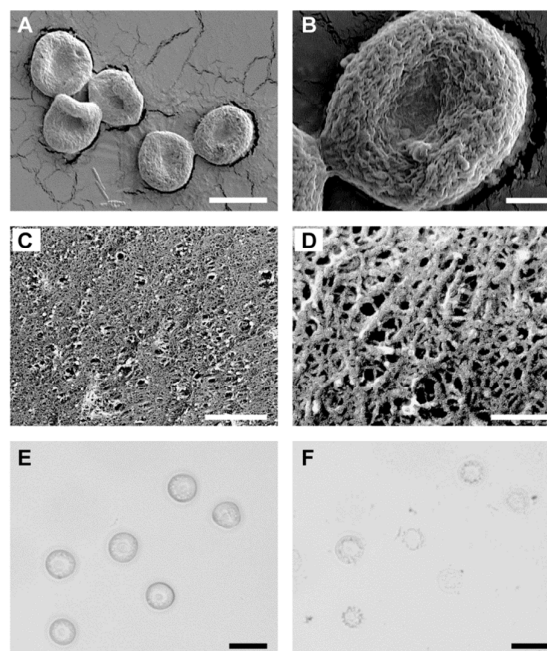


Figure 5. (A, B) SEM images of the collagen particles prepared using microfluidic devices. (C, D) FF-TEM images of the cross section of the collagen particles with different magnifications. (E, F) Digestion of collagen particles by collagenase; particles were dipped in a collagenase solution for (E) 0 and (F) 2 h. Scale bars: (A) 10 μm, (B) 2 μm, (C) 500 nm, (D) 100 nm, and (E, F) 20 μm.

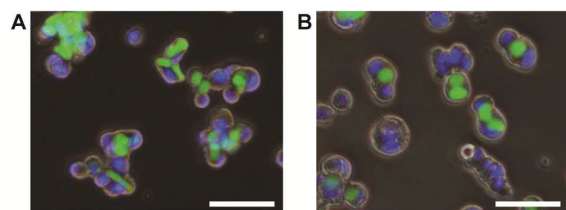


Figure 6. Cell adhesion on the collagen particles. (A) NIH-3T3 cells and (B) HepG2 cells cultured on a non-cell-adhesive dish with collagen particles for 3 and 6 h, respectively. FITC-labeled collagen was incorporated in the particles. Cell nuclei were stained blue using Hoechst 33342. Scale bar, 50 μm .

cell-cell interactions on cellular functions.

Figure 7 (B) shows the agarose hydrogel microchambers (diameter = 200 μm , depth = 300 μm) with introduced cells and particles. Cells and particles formed aggregates after just 1 day of cultivation. Aggregate size further decreased with the progress of the cell cultivation until day 7 (Fig. 7 (B)) due to the cell/cell and cell/particle contraction forces. Because the agarose hydrogel chambers are non-cell-adhesive, we were easily able to recover the formed spheroids from the chamber by gentle centrifugation (Fig. 7 (C)). The aggregates were not perfectly spherical, especially those in the high particle ratio condition. Cylindrical aggregates, corresponding to the chamber morphology, were formed as a result of the relatively low contraction forces between cells. From fluorescence observation of the particles prepared using FITC-labeled collagen, we were able to confirm that the particles were randomly dispersed within the spheroids.

Characterization and function analysis of composite spheroids

The cross sectional morphology of the composite spheroids was examined by immunohistochemistry. Figure 8 shows thin sections of the composite spheroids taken after 14 days of cultivation. In the composite spheroids, collagen particles were observed between hepatocytes that produce albumin. Collagen particles were almost randomly dispersed within the spheroids, not forming aggregates. The hepatocyte functions in the composite spheroids were further examined by quantitative PCR and compared to those seen in the case of conventional plate culture and spheroid culture without incorporating collagen particles. Figure 9 shows the expression of hepatocyte-specific genes after 7 days of cultivation. Compared to the findings obtained in the case of conventional plate culture on a collagen-coated dish, the expression of all of these genes was upregulated for the spheroid culture conditions, with/without the incorporation of collagen particles. Under the spheroid culture conditions, the expression of ALB (albumin) and OTC (ornithine transcarbamylase, associated with urea synthesis) was the highest with a cell and particle ratio of 1:1, indicating that there is an optimal ratio for upregulating these genes. The differences in the expression of *CYP3A1* (cytochrome P450 3A1, associated with drug metabolism in rats) among the spheroid cultivations were not statistically significant, but the

highest expression level was observed for the particle:cell = 4:1 condition, indicating that the cellular microenvironment was changed by the presence of the collagen particles.

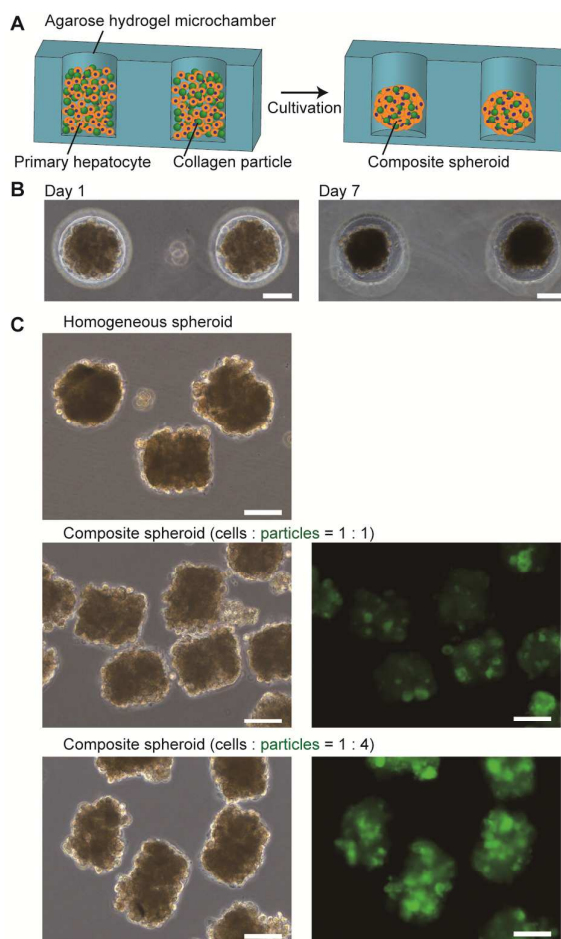


Figure 7. Formation of composite spheroids of primary rat hepatocytes, incorporating collagen particles. (A) Schematic showing the formation of composite spheroids using a non-cell-adhesive microchamber made of agarose hydrogel. (B) Spheroids formed within the microwells at days 1 and 7, when the cell:particle ratio was 1:1. (C) Bright-field and fluorescence images of the homogeneous and composite spheroids recovered from the microchambers at day 7. The ratio of cells and particles was changed as indicated. Collagen particles incorporating FITC-labeled collagen were used. Scale bar, 100 μm .

Discussion

Collagen is the most abundant protein in our body. It plays critical roles in maintaining cellular morphology and functions such as differentiation and proliferation, through interactions with cell surface and ECM molecules. Collagen has become an essential material for biomedical applications, especially in the fields of tissue engineering and mammalian cell cultivation^{40,41}. For instance, the sandwich cultivation of hepatocytes between collagen hydrogel layers enables the long-term maintenance of cellular functions⁴². In addition, cell culture platforms utilizing collagen-based scaffolds and collagen-coated surfaces have

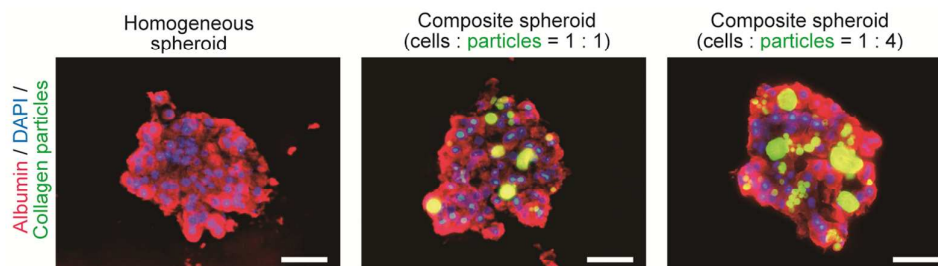


Figure 8. Immunofluorescent staining of the composite spheroids of primary hepatocytes at day 14. Albumin was stained red (hepatocytes). Scale bar, 50 μm .

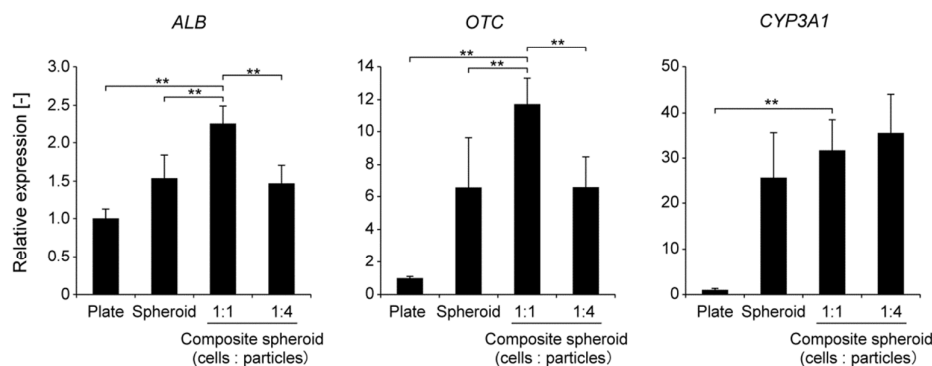


Figure 9. Expression of hepatocyte-specific genes determined by quantitative PCR, analyzed at day 7. *ALB*: albumin, *OTC*: ornithine transcarbamylase, *CYP3A1*: cytochrome P450 3A1. *ATP5F1* was used as the internal control. Plate: hepatocytes cultured on a collagen-coated dish, Spheroid: homogeneous spheroids without incorporating collagen particles, Composite spheroids: spheroids incorporating collagen particles. ** $p < 0.01$.

been often used, including porous or fibrous scaffolds of collagen^{43,44} and collagen vitrigels⁴⁵. Collagen particles, such as growth factor-releasing particles, have been produced and used as drug loading carriers for regenerative medicine^{29,30}. However, the preparation of condensed collagen microparticles, with sizes similar to those of single cells, has proven more difficult. This is mainly because of the difficulty of manipulating a highly viscous collagen solution at a high concentration. In addition, particle size and distribution cannot be precisely controlled when bulk scale techniques are employed for producing collagen particles, such as conventional emulsification.

In contrast, here we present novel processes that enable the formation of condensed collagen particles. Utilizing the dissolution of droplets in a non-equilibrium state, we obtained collagen particles with an estimated final concentration higher than 10%, despite using 0.01–0.2% collagen solutions. The precise control of the formation and dissolution of aqueous droplets of collagen in a polar organic solvent cannot be realized if droplet microfluidics is not employed. As a result, the particles obtained were sufficiently stable for cell cultivation, in spite of their small sizes. The microfluidic process presented here allows precise control of the size of the particles, while the membrane-emulsification technique can be used to produce a relatively large amount of particles ($\sim 3 \times 10^7$ particles per hour). The TEM observation of the cross sectional morphologies revealed that the particles were

composed of closely packed narrow collagen fibers with diameters of 10–20 nm. It is known that collagen molecules have an ability to self-assemble into highly organized supramolecular fibrils. In literatures, the fibril diameter of type I collagen reconstituted in vitro can be controlled by changing the collagen concentration and the ionic strength and pH of the solution, and it typically ranges from 10 nm to several micrometers^{46,47}. The relatively small diameter of the collagen fibers in the particles prepared was mostly due to the high collagen concentration within the shrunk droplet and the short time period until the crosslinking reaction.

The transformation of a collagen solution into cell-sized particles generates numerous advantages for tissue engineering. First, such particles can be uniformly incorporated into 3D cell culture scaffolds. Various types of 3D cell culture techniques have been reported, including spheroid formation, usage of sponge type or fibrous scaffolds, cell seeding into decellularized organs, and cell encapsulation into hydrogels. However, it has previously been difficult to uniformly introduce cells into relatively large porous scaffolds composed of ECM molecules. In addition, the degree of cell-cell contact and cell-matrix interaction cannot be freely controlled by the conventional processes of spheroid formation and hydrogel culture. By adopting our approach based on particulate ECM, we are able to regenerate cell-ECM interactions and assemble cells and particles into 3D constructs with a uniform particle distribution, through the

simple process of spheroid formation. Second, the particles prepared in this study were small and had a relatively high surface-to-volume ratio, thus enabling the efficient adhesion of multiple particles to one cell when composite spheroids were formed. Although we mainly used $\sim 10\text{-}\mu\text{m}$ -sized particles, it will soon be possible to produce particles with much smaller sizes, when narrow microchannels or membranes with small pores are used, or a further diluted collagen solution is employed. Third, the particles are highly condensed and solid and are therefore stable in 3D culture and show stable cell adhesion on their surface; we did not observe the deformation or degradation of collagen particles during the spheroid culture for 2 weeks.

In the present study, we demonstrate the formation of composite spheroids of primary hepatocytes. Isolated hepatocytes are essential for various medical, biochemical, and pharmacological applications, including cell-based drug screening assays⁴⁸, the preparation of bioartificial liver devices for acute liver failure⁴⁹, and the construction of transplantable hepatic constructs⁵⁰. Although the liver has an extremely high regeneration ability in vivo, it is highly difficult to maintain the functions and viability of isolated hepatocytes under culture conditions. One of the reasons for this is the high complexity of liver microstructures (in particular, the sinusoidal structure). In the liver, hepatocytes are radially aligned in one row around the central vein and surrounded by sinusoidal endothelial cells through a thin layer containing ECM components, stellate cells, and plasma components, called the space of Disse⁵¹. That is, hepatocytes are connected with other hepatocytes through the apical side, whereas the basolateral side faces ECM components. Hence, both cell-cell and cell-matrix interactions are important for hepatocytes. In conventional spheroid formation, which uses hepatocytes alone, close cell-cell contacts are formed but in vivo cell-ECM interactions are very difficult to reconstruct. In this study, we demonstrated that hepatocyte functions are upregulated in the presence of collagen microparticles in the spheroids of primary hepatocytes, likely due to the addition of cell-matrix contacts in the packed cell aggregates. In addition, we demonstrated that there exists an optimal ratio of cells and particles; in the case of a higher number of particles (cells: particles = 1:4) hepatocyte functions were reduced compared to the lower particle condition (particles: cells = 1:1). This suggests that cell-cell contacts became scarce in the high particle-ratio condition.

The composite spheroids discussed here would be useful as a tool for drug screening and evaluation, as hepatocytes play essential roles in drug metabolism. To date, attempts have only been made to study the drug-metabolizing activities of hepatocytes using spheroid culture, aiming to realize an in vivo-like environment for reliable evaluations. These composite spheroids would be useful, not only because of the upregulation of cellular functions but also due to the ease of the preparation process. Various techniques would be available to form spheroids, including non-cell-adhesive dishes, hanging drop cell cultures, microwell plates, and recently reported microfluidic devices and microfabricated chambers⁵⁻

⁸. In this study, we demonstrated the application of type I collagen particles, prepared by the condensation of droplets and subsequent crosslinking with glutaraldehyde, to the preparation of composite spheroids of hepatocytes. However, we did not optimize the various physicochemical parameters of the particles for upregulating hepatic functions. Future studies would include the search for the suitable conditions, including particle size, shape, composition, the use of other crosslinking reagents or strategies, and the size and diameter of the reconstituted collagen nanofibers composing the particles. In particular, different collagen types would be critical for regulating hepatocyte functions, because the liver includes four types of collagens (collagen type I, III, IV, and V)⁵². Hence, the search for and optimization of different types of collagen would be beneficial to cellular function. Furthermore, the preparation of functional particles, such as growth factor loading particles, would widen the application range of the particles even further. Finally, the formation of multicellular spheroids from other types of cells could also be possible, including ECM particle encapsulating embryoid bodies and neurospheres.

Conclusions

We have demonstrated the production of cell-sized collagen microparticles using microfluidic processes and membrane emulsification. Composite spheroids of primary hepatocytes were formed, and hepatocyte-specific functions were upregulated when the ratios of the particles and cells were equal. Our approach of using collagen microparticles as particulate scaffolds for 3D tissue engineering will be advantageous because of its ability to preserve cellular functions, simplicity of operation, and high versatility.

Acknowledgments

This study was supported in part by Grants-in-Aid for Scientific Research on Innovative Areas (Hyper BioAssembler Project, M.S. no. 23106007; M.Y.(2) no. 23106009), for Young Scientist (M.Y.(1) no. 25750171), for Scientific Research C (R.U. no. 26350530) and for JSPS Fellows (Y.Y.) from the Ministry of Education, Culture, Sports, Science, and Technology of Japan.

References

1. F. Pampaloni, E. G. Reynaud and E. H. K. Stelzer, *Nat. Rev. Mol. Cell. Biol.*, 2007, **8**, 839-845.
2. S. F. Wong, Y. No da, Y. Y. Choi, D. S. Kim, B. G. Chung and S. H. Lee, *Biomaterials*, 2011, **32**, 8087-8096.
3. J. M. Kelm, N. E. Timmins, C. J. Brown, M. Fussenegger and L. K. Nielsen, *Biotechnol. Bioeng.*, 2003, **83**, 173-180.
4. J. Fukuda, A. Khademhosseini, Y. Yeo, X. Y. Yang, J. Yeh, G. Eng, J. Blumling, C. F. Wang, D. S. Kohane and R. Langer, *Biomaterials*, 2006, **27**, 5259-5267.
5. F. Ozawa, K. Ino, T. Arai, J. Ramon-Azcon, Y. Takahashi, H. Shiku and T. Matsue, *Lab Chip*, 2013, **13**, 3128-3135.

6. H. Ota, T. Kodama and N. Miki, *Biomicrofluidics*, 2011, **5**, 34105.
7. H. J. Jin, Y. H. Cho, J. M. Gu, J. Kim and Y. S. Oh, *Lab Chip*, 2011, **11**, 115-119.
8. S. A. Lee, D. Y. No, E. Kang, J. Ju, D. S. Kim and S. H. Lee, *Lab Chip*, 2013, **13**, 3529-3537.
9. R. Kojima, K. Yoshimoto, E. Takahashi, M. Ichino, H. Miyoshi and Y. Nagasaki, *Lab Chip*, 2009, **9**, 1991-1993.
10. H. Hardelauf, J. P. Frimat, J. D. Stewart, W. Schormann, Y. Y. Chiang, P. Lampen, J. Franzke, J. G. Hengstler, C. Cadenas, L. A. Kunz-Schughart and J. West, *Lab Chip*, 2011, **11**, 419-428.
11. S. H. Moon, J. Ju, S. J. Park, D. Bae, H. M. Chung and S. H. Lee, *Biomaterials*, 2014, **35**, 5987-5997.
12. M. A. Kinney, T. A. Hookway, Y. Wang and T. C. McDevitt, *Ann. Biomed. Eng.*, 2014, **42**, 352-367.
13. J. Seo, J. S. Lee, K. Lee, D. Kim, K. Yang, S. Shin, C. Mahata, H. B. Jung, W. Lee, S. W. Cho and T. Lee, *Adv. Mater.*, 2014, **26**, 7043-7050.
14. S. F. Abu-Absi, L. K. Hansen and W. S. Hu, *Cytotechnology*, 2004, **45**, 125-140.
15. Y. J. Choi, J. Park and S. H. Lee, *Biomaterials*, 2013, **34**, 2938-2946.
16. H. Tanaka, S. Tanaka, K. Sekine, S. Kita, A. Okamura, T. Takebe, Y. W. Zheng, Y. Ueno, J. Tanaka and H. Taniguchi, *Biomaterials*, 2013, **34**, 5785-5791.
17. Y. Jun, M. J. Kim, Y. H. Hwang, E. A. Jeon, A. R. Kang, S. H. Lee and D. Y. Lee, *Biomaterials*, 2013, **34**, 8122-8130.
18. R. Paduch, A. Walter-Croneck, B. Zdzisinska, A. Szuster-Ciesielska and M. Kandefer-Szerszen, *Cell Biol. Intern.*, 2005, **29**, 497-505.
19. Y. S. Torisawa, H. Shiku, T. Yasukawa, M. Nishizawa and T. Matsue, *Biomaterials*, 2005, **26**, 2165-2172.
20. A. Ivascu and M. Kubbies, *J. Biomol. Screen.*, 2006, **11**, 922-932.
21. K. Kwapiszewska, A. Michalczyk, M. Rybka, R. Kwapiszewski and Z. Brzozka, *Lab Chip*, 2014, **14**, 2096-2104.
22. J. Ruppen, L. Cortes-Dericks, E. Marconi, G. Karoubi, R. A. Schmid, R. Peng, T. M. Marti and O. T. Guenat, *Lab Chip*, 2014, **14**, 1198-1205.
23. T. Takezawa, M. Yamazaki, Y. Mori, T. Yonaha and K. Yoshizato, *J. Cell Sci.*, 1992, **101**, 495-501.
24. M. Yamada, R. Utoh, K. Ohashi, K. Tatsumi, M. Yamato, T. Okano and M. Seki, *Biomaterials*, 2012, **33**, 8304-8315.
25. A. Kobayashi, K. Yamakoshi, Y. Yajima, R. Utoh, M. Yamada and M. Seki, *J. Biosci. Bioeng.*, 2013, **116**, 761-767.
26. D. M. Dean, A. P. Napolitano, J. Youssef and J. R. Morgan, *FASEB J.*, 2007, **21**, 4005-4012.
27. Y. T. Matsunaga, Y. Morimoto and S. Takeuchi, *Adv. Mater.*, 2011, **23**, H90-94.
28. S. L. Friedman, F. J. Roll, J. Boyles and D. M. Bissell, *Proc. Natl. Acad. Sci. U. S. A.*, 1985, **82**, 8681-8685.
29. O. C. Chan, K. F. So and B. P. Chan, *J. Control. Rel.*, 2008, **129**, 135-143.
30. N. Nagai, N. Kumasaka, T. Kawashima, H. Kaji, M. Nishizawa and T. Abe, *J. Mater. Sci. Mater. Med.*, 2010, **21**, 1891-1898.
31. L. Yao, F. Phan and Y. Li, *Stem Cell Res. Ther.*, 2013, **4**, 109.
32. T. Muthukumar, D. Sankari, A. Tamil Selvi and T. P. Sastry, *J. Mater. Sci.*, 2014, **49**, 5730-5737.
33. S. Hong, H. J. Hsu, R. Kaunas and J. Kameoka, *Lab Chip*, 2012, **12**, 3277-3280.
34. H. Wang, S. C. Leeuwenburgh, Y. Li and J. A. Jansen, *Tissue Eng. Part B*, 2012, **18**, 24-39.
35. S. Sugaya, M. Yamada, A. Hori and M. Seki, *Biomicrofluidics*, 2013, **7**, 54120.
36. T. Ono, M. Yamada, Y. Suzuki, T. Taniguchi and M. Seki, *RSC Adv.*, 2014, **4**, 13557.
37. D. C. Duffy, J. C. McDonald, O. J. Schueller and G. M. Whitesides, *Anal. Chem.*, 1998, **70**, 4974-4984.
38. P. O. Seglen, *Methods Cell Biol.*, 1976, **13**, 29-83.
39. C. Charcosset, I. Limayem and H. Fessi, *J. Chem. Technol. Biot.*, 2004, **79**, 209-218.
40. C. H. Lee, A. Singla and Y. Lee, *Int. J. Pharm.*, 2001, **221**, 1-22.
41. J. Glowacki and S. Mizuno, *Biopolymers*, 2008, **89**, 338-344.
42. J. C. Dunn, R. G. Tompkins and M. L. Yarmush, *J. Cell Biol.*, 1992, **116**, 1043-1053.
43. J. A. Matthews, G. E. Wnek, D. G. Simpson and G. L. Bowlin, *Biomacromolecules*, 2002, **3**, 232-238.
44. E. Sachlos, N. Reis, C. Ainsley, B. Derby and J. T. Czernuszka, *Biomaterials*, 2003, **24**, 1487-1497.
45. T. Takezawa, K. Ozaki, A. Nitani, C. Takabayashi and T. Shimo-Oka, *Cell Transplant.*, 2004, **13**, 463-473.
46. G. Mosser, A. Anglo, C. Helary, Y. Bouligand and M. M. Giraud-Guille, *Matrix Biol.*, 2006, **25**, 3-13.
47. F. Gobeaux, G. Mosser, A. Anglo, P. Panine, P. Davidson, M. M. Giraud-Guille and E. Belamie, *J. Mol. Biol.*, 2008, **376**, 1509-1522.
48. S. R. Khetani and S. N. Bhatia, *Nat. Biotechnol.*, 2008, **26**, 120-126.
49. J. W. Allen, T. Hassanein and S. N. Bhatia, *Hepatology*, 2001, **34**, 447-455.
50. K. Ohashi, T. Yokoyama, M. Yamato, H. Kuge, H. Kanehiro, M. Tsutsumi, T. Amanuma, H. Iwata, J. Yang, T. Okano and Y. Nakajima, *Nat. Med.*, 2007, **13**, 880-885.
51. E. Wisse, R. B. Dezanger, K. Charels, P. Vandersmissen and R. S. Mccuskey, *Hepatology*, 1985, **5**, 683-692.
52. R. S. Aycock and J. M. Seyer, *Connect. Tissue Res.*, 1989, **23**, 19-31.

Graphical Abstract

for

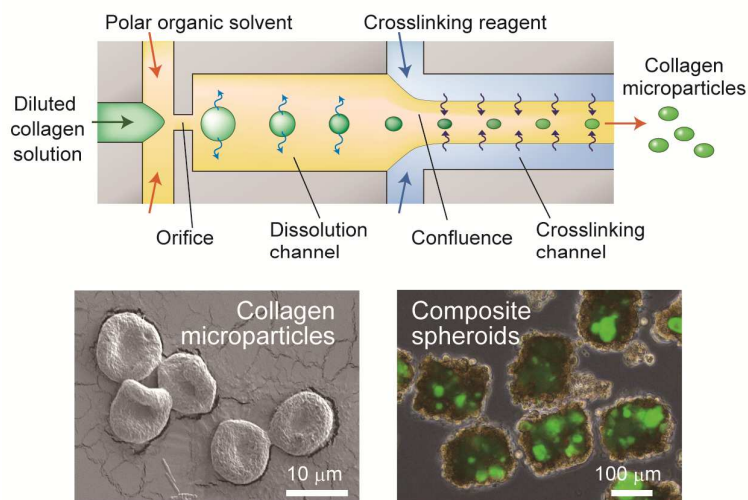
Cell-sized condensed collagen microparticles for preparing
microengineered composite spheroids of primary hepatocytes

Masumi Yamada,^{a,*} Ayaka Hori,^a Sari Sugaya,^a Yuya Yajima,^a Rie Utoh,^b Masayuki Yamato,^b and Minoru Seki^a

^aDepartment of Applied Chemistry and Biotechnology, Graduate School of Engineering, Chiba University, 1-33 Yayoi-cho, Inage-ku, Chiba 263-8522, Japan.

^bInstitute of Advanced Biomedical Engineering and Science, Tokyo Women's Medical University, 8-1 Kawada-cho, Shinjuku-ku, Tokyo 162-8666, Japan.

*E-mail: m-yamada@faculty.chiba-u.jp; Tel/fax: +81-43-290-3398



Cell-sized, highly condensed collagen microparticles were produced, which were utilized to fabricate composite multicellular spheroids of primary hepatocytes.